Available online at www.sciencedirect.com
ScienceDirect
International Journal of Heat and Mass Transfer 50 (2007) 2643–2655
International Journal of HEAT and MASS TRANSFER
www.elsevier.com/locate/ijhmt

Use of extended Kalman filtering in detecting fouling in heat exchangers

Gudmundur R. Jonsson [a], Sylvain Lalot [b,*], Olafur P. Palsson [a], Bernard Desmet [b]

[a] Department of Mechanical and Industrial Engineering, University of Iceland, Hjardarhaga 2-4, 107 Reykjavik, Iceland
[b] LME, Université de Valenciennes et du Hainaut Cambrésis, Le Mont Houy, 59313 Valenciennes Cedex, France

Received 31 August 2006; received in revised form 23 November 2006
Available online 17 January 2007

Abstract

This paper is concerned with how non-linear physical state space models can be applied to on-line detection of fouling in heat exchangers. The model parameters are estimated by using an extended Kalman filter and measurements of inlet and outlet temperatures and mass flow rates. In contrast to most conventional methods, fouling can be detected when the heat exchanger operates in transient states. Measurements from a clean counterflow heat exchanger are first used to optimize the Kalman filter. Then fouling is considered. The results show that the proposed method is very sensitive, hence well suited for fouling detection.

Keywords: Heat exchangers; Fouling; Extended Kalman filter; Parameter estimation; On-line detection

1. Introduction

The heat transfer between two fluids will inevitably result in fouling. For a district heating system, where the heat transfer is great, it is important to minimise fouling in the heat exchangers. The expense for achieving a desired heat transfer is increased with the decrease of the heat transfer coefficient. For example, at the Vestegnens Kraftvarmeselskab in Denmark (VEKS), it is said, that for every 5° temperature increase for which the hot water flowing into the heat exchangers must be heated because of fouling, is an added 800–940 k€/year cost for the consumers, see Jakobsen and Stampe [1]. The installed power at VEKS is 770 MW which is similar to that of the District Heating Company of Reykjavik, Iceland. From the environmental point of view, fouling is also harmful. For example, Casanueva-Robles and Bott [2] report that a fouling biofilm thickness of 200 μm in a 550 MW coal-fired power station leads to about an increase by 12 tons of CO_2 per day.

Causes for fouling, common methods to avoid it, or at least to mitigate it, have long been studied, see for example Poulsen [3], Thonon et al. [4], Ramachandra et al. [5], and Abd-Elhady et al. [6]. The detection of the presence of fouling is also an active research area, see for example Jerónimo et al. [7], Bott [8], Riverol and Napolitano [9,10], Chen et al. [11], Nema and Datta [12] and is still a challenge and conferences are regularly organized (see for example http://www.engconfintl.org/).

The classical detection methods are based on e.g.

1. Examination of the heat transfer coefficient (or the effectiveness),
2. simultaneous observations of pressure drops and mass flow rates,
3. temperature measurements, e.g. $(T_{h,in} - T_{h,out})/(T_{h,in} - T_{h,out})_{design}$,
4. ultrasonic or electrical measurements,
5. weighing of heat exchanger plates.

To be very accurate, these methods require either that the system presents successive steady states (1–3), i.e. the

* Corresponding author. Tel.: +33 327 511 973; fax: +33 327 511 960.
E-mail addresses: grj@hi.is (G.R. Jonsson), sylvain.lalot@univ-valenciennes.fr (S. Lalot), opp@hi.is (O.P. Palsson), bernard.desmet@univ-valenciennes.fr (B. Desmet).

0017-9310/$ - see front matter © 2006 Elsevier Ltd. All rights reserved.
doi:10.1016/j.ijheatmasstransfer.2006.11.025

Nomenclature

A	state matrix or surface area for heat transfer when used with a subscript
B	state matrix
Cus	cumulative sum function
c	constant or specific heat when used with a subscript
$\frac{\mathrm{d}}{\mathrm{d}t}$	derivative with respect to time
$\frac{\partial}{\partial v}$	partial derivative with respect to variable v
$E[v]$	mean value of variable v
F	state matrix
$\underline{f}$	state space function
$\underline{g}$	threshold coefficient
H	measurement matrix
h	threshold coefficient or convection coefficient when used with a subscript
I	identity matrix
K	Kalman gain matrix or constant when used with subscripts c or h
k	discrete time index
M	mass of fluid in one section
$\dot{m}$	mass flow rate
$\underline{\dot{m}}$	mass flow rate state vector
N	normal (Gaussian) distribution
ns	number of sections in the heat exchanger
P	covariance error matrix
Q	covariance matrix
R_f	fouling factor
R_th	thermal resistance of the tube between the two fluids
T	temperature
$\underline{T}$	temperature state vector
t	time
U	overall heat transfer coefficient
v	dummy variable
w	white Gaussian noise sequence with zero mean and covariance matrix Q
$\underline{w}$	noise state vector
$\underline{x}$	overall state vector
y	exponent of the Reynolds number in a convection correlation
$\underline{z}$	measurements vector
$0(m \times n)$	null matrix having m lines and n columns
$\underline{0}$	null state vector

Greek symbols

α	model parameter
β	model parameter
Δt	time step
$\underline{\theta}$	parameter state vector
σ	standard deviation
τ	model parameter

Subscripts

c	cold side
design	as should be obtained according to the design computations
f	relative to the state space function
h	hot side
i	in section #i
in	inlet
k	at discrete time index k
out	outlet
ref	reference
z	relative to the measurements
α	relative to the model parameter α
β	relative to the model parameter β
θ	relative to the parameter state vector

Superscripts

*	relative to the reference state
T	transpose

inlet temperatures and flows must be stable for a period long enough to be able to compute or measure the values of interest, or are local (4), or require to stop the process (5). This is far too restrictive or costly.

Another approach is based on modelling the heat exchanger and then looking for any discrepancy between what is predicted by the model and what actually occurs. The method proposed by Prieto et al. [13,14] is based on an adaptation of the model when necessary (after the detection of the discrepancy), and on the analysis of the differences between two consecutive models. To pursue this approach, the aim of the present study is to show how non-linear physical state space models, recursively determined, can be applied to detect fouling in heat exchangers. In Jonsson and Holst [15] and Jonsson [16] heat exchanger models and the statistical estimation of their parameters are discussed. The models are based on the physical properties of the heat exchanger. An improvement has been brought so that the estimation is continuous, and the main focus here is to determine how sensitive the proposed method is to changes in the parameters of the model due to fouling.

Being based on the measurements of the mass flow rates and on the inlet/outlet temperatures, the estimation could be done while the heat exchanger is in use, even in a non steady state.

In the first part, the heat exchanger model is developed. Then the estimation algorithm is presented. This estimation is carried out using the extended Kalman filter. The last section is split into two subsections. The first subsection

is devoted to the tuning of the Kalman filter, to the study of the influence of the initial random conditions, and the influence of the sampling period. This is carried out on a clean heat exchanger. The second subsection deals with the application of the model, coupled to a drift detection tool to fouling detection.

2. The heat exchanger model

2.1. The model

The heat exchanger model is based on the direct lumping of the process. The heat exchanger is split up into sections (in the axial direction of the exchanger), each section being a set of two cells, one per fluid. The temperature in each section is a model state. An extensive discussion of the derivation and assumptions of this model is given in Jonsson and Palsson [17].

It can be shown that two sections are sufficient, even though the number of cells in the model may of course be increased, cf. Jonsson [16]. In this case, the equation representing the model is

$$\frac{\mathrm{d}}{\mathrm{d}t}\begin{bmatrix} T_{\mathrm{h},1} \\ T_{\mathrm{h},2} \\ T_{\mathrm{c},1} \\ T_{\mathrm{c},2} \end{bmatrix} = \begin{bmatrix} -\left(1+\frac{\alpha}{2}\right)/\tau_{\mathrm{h}} & 0 & \frac{\alpha}{2\tau_{\mathrm{h}}} & \frac{\alpha}{2\tau_{\mathrm{h}}} \\ \left(1-\frac{\alpha}{2}\right)/\tau_{\mathrm{h}} & -\left(1+\frac{\alpha}{2}\right)/\tau_{\mathrm{h}} & \frac{\alpha}{2\tau_{\mathrm{h}}} & 0 \\ \frac{\beta}{2\tau_{\mathrm{c}}} & \frac{\beta}{2\tau_{\mathrm{c}}} & -\left(1+\frac{\beta}{2}\right)/\tau_{\mathrm{c}} & 0 \\ \frac{\beta}{2\tau_{\mathrm{c}}} & 0 & \left(1-\frac{\beta}{2}\right)/\tau_{\mathrm{c}} & -\left(1+\frac{\beta}{2}\right)/\tau_{\mathrm{c}} \end{bmatrix} \times \begin{bmatrix} T_{\mathrm{h},1} \\ T_{\mathrm{h},2} \\ T_{\mathrm{c},1} \\ T_{\mathrm{c},2} \end{bmatrix} + \begin{bmatrix} \left(1-\frac{\alpha}{2}\right)/\tau_{\mathrm{h}} & 0 \\ 0 & \frac{\alpha}{2\tau_{\mathrm{h}}} \\ 0 & \left(1-\frac{\beta}{2}\right)/\tau_{\mathrm{c}} \\ \frac{\beta}{2\tau_{\mathrm{c}}} & 0 \end{bmatrix} \begin{bmatrix} T_{\mathrm{h,in}} \\ T_{\mathrm{c,in}} \end{bmatrix} \tag{1}$$

where $T_{\mathrm{h},1}$, temperature in hot section #1; $T_{\mathrm{h},2}$, temperature in hot section #2 = outlet temperature of the hot fluid; $T_{\mathrm{c},1}$, temperature in cold section #1; $T_{\mathrm{c},2}$, temperature in cold section #2 = outlet temperature of the cold fluid; $\alpha, \beta, \tau_{\mathrm{h}}$ and τ_{c} are model parameters. They are time dependent as they are functions of the mass flow rates. In addition α and β may also be temperature dependent, but this will not be considered here, due to the fact that the thermophysical characteristics of the fluids are considered constant in the CFD code.

Generally the models may be written as

$$\frac{\mathrm{d}}{\mathrm{d}t}\underline{T} = A(\underline{\dot{m}}, \underline{T}, \underline{\theta})\underline{T} + B(\underline{\dot{m}}, \underline{T}, \underline{\theta})\underline{T}_{\mathrm{in}} \tag{2}$$

or

$$\frac{\mathrm{d}}{\mathrm{d}t}\underline{T} = \underline{f}(\underline{\dot{m}}, \underline{T}, \underline{\theta}, \underline{T}_{\mathrm{in}}) \tag{3}$$

where $\underline{\dot{m}} = [\dot{m}_{\mathrm{h}}\ \dot{m}_{\mathrm{c}}]^{\mathrm{T}}$, $\underline{T}_{\mathrm{in}} = [T_{\mathrm{h,in}}\ T_{\mathrm{c,in}}]^{\mathrm{T}}$, $\underline{T}$ contains the temperature in each section, and the model parameters are contained in the state vector $\underline{\theta}$.

2.2. The parameterization

The models contain four basic parameters which are given by

$$\alpha(t) = \frac{A_{\mathrm{h}}U}{\dot{m}_{\mathrm{h}}(t)c_{\mathrm{h}}}, \quad \tau_{\mathrm{h}}(t) = \frac{M_{\mathrm{h}}}{\dot{m}_{\mathrm{h}}(t)},$$
$$\beta(t) = \frac{A_{\mathrm{c}}U}{\dot{m}_{\mathrm{c}}(t)c_{\mathrm{c}}}, \quad \tau_{\mathrm{c}}(t) = \frac{M_{\mathrm{c}}}{\dot{m}_{\mathrm{c}}(t)} \tag{4}$$

α and β are dimensionless, they are the instantaneous values of the number of transfer units, for the hot and cold side respectively, but τ_{h} and τ_{c} are given in seconds. In a first step, and to introduce reference values, it is assumed that U in Eq. (4) is a constant and hence the parameters are only flow dependent as shown in Eq. (5). To link the parameters to some reference state ($*$) they are scaled as follows (U now written as U^*).

$$\begin{aligned} \alpha(t) &= \frac{U^*A_{\mathrm{h}}}{\dot{m}^*_{\mathrm{h}}c_{\mathrm{h}}}\frac{\dot{m}^*_{\mathrm{h}}}{\dot{m}_{\mathrm{h}}(t)} = \alpha^*\frac{\dot{m}^*_{\mathrm{h}}}{\dot{m}_{\mathrm{h}}(t)}, \\ \tau_{\mathrm{h}}(t) &= \frac{M_{\mathrm{h}}}{\dot{m}^*_{\mathrm{h}}}\frac{\dot{m}^*_{\mathrm{h}}}{\dot{m}_{\mathrm{h}}(t)} = \tau^*_{\mathrm{h}}\frac{\dot{m}^*_{\mathrm{h}}}{\dot{m}_{\mathrm{h}}(t)}, \\ \beta(t) &= \frac{U^*A_{\mathrm{c}}}{\dot{m}^*_{\mathrm{c}}c_{\mathrm{c}}}\frac{\dot{m}^*_{\mathrm{c}}}{\dot{m}_{\mathrm{c}}(t)} = \beta^*\frac{\dot{m}^*_{\mathrm{c}}}{\dot{m}_{\mathrm{c}}(t)}, \\ \tau_{\mathrm{c}}(t) &= \frac{M_{\mathrm{c}}}{\dot{m}^*_{\mathrm{c}}}\frac{\dot{m}^*_{\mathrm{c}}}{\dot{m}_{\mathrm{c}}(t)} = \tau^*_{\mathrm{c}}\frac{\dot{m}^*_{\mathrm{c}}}{\dot{m}_{\mathrm{c}}(t)} \end{aligned} \tag{5}$$

The reference state is arbitrary, i.e. the parameters

$$\theta^* = \left\{\alpha^*, \tau^*_{\mathrm{h}}, \beta^*, \tau^*_{\mathrm{c}}\right\}^{\mathrm{T}} \tag{6}$$

are constants.

In Jonsson and Palsson [17] it is shown that considerable enhancements in modelling are obtained when U is assumed mass flow dependent. Further improvements can be made when U is also temperature dependent. As already mentioned, the fluid characteristics have been considered constant in the CFD code, so this temperature dependency of U will not be used here.

For both sides of the heat exchanger used here, the convection coefficients, h_{h} and h_{c} are (see e.g. [18] or [19]):

$$h_{\mathrm{h}}(t) = K_{\mathrm{h}}\dot{m}^{y_{\mathrm{h}}}_{\mathrm{h}}(t), \quad h_{\mathrm{c}}(t) = K_{\mathrm{c}}\dot{m}^{y_{\mathrm{c}}}_{\mathrm{c}}(t) \tag{7}$$

where K_{h}, K_{c}, y_{h} and y_{c} are constants. In the present study, the fluids flow in either a circular tube or in the annulus, the flow regime is always turbulent in all experiments for both fluids, and the entrance effect length is negligible compared to the length of the heat exchanger. Hence, it is considered here that y_{h} and y_{c} can be taken as $y_{\mathrm{h}} = y_{\mathrm{c}} = y = 0.8$ (see e.g. [20]).

In this study, the thermal conductive resistance as well as the thermal inertia of the tube are neglected (but could have been taken into account in the model [21]), but the heat exchange areas are considered different (as should be necessary for finned tube heat exchangers), and are respectively based on the inner and outer radius of the tube. So,

the overall heat transfer coefficient can be computed using $1/(UA_{\mathrm{ref}}) \cong 1/(h_{\mathrm{h}}A_{\mathrm{h}}) + 1/(h_{\mathrm{c}}A_{\mathrm{c}})$, where A_{ref} can be arbitrary chosen as the heat exchange area of the cold side or of the hot side. This leads to:

$$A_{\mathrm{ref}}U(t) = \frac{A_{\mathrm{h}}h_{\mathrm{h}}(t)A_{\mathrm{c}}h_{\mathrm{c}}(t)}{A_{\mathrm{h}}h_{\mathrm{h}}(t) + A_{\mathrm{c}}h_{\mathrm{c}}(t)} = \frac{A_{\mathrm{h}}A_{\mathrm{c}}K_{\mathrm{h}}K_{\mathrm{c}}(\dot{m}_{\mathrm{h}}(t)\dot{m}_{\mathrm{c}}(t))^{y}}{A_{\mathrm{c}}K_{\mathrm{c}}\dot{m}_{\mathrm{c}}^{y}(t) + A_{\mathrm{h}}K_{\mathrm{h}}\dot{m}_{\mathrm{h}}^{y}(t)} \quad (8)$$

The overall heat transfer coefficient at the reference mass flows, $\dot{m}_{\mathrm{h}}^{*}$ and $\dot{m}_{\mathrm{c}}^{*}$, is similarly

$$A_{\mathrm{ref}}U^{*} = \frac{A_{\mathrm{h}}A_{\mathrm{c}}K_{\mathrm{h}}K_{\mathrm{c}}(\dot{m}_{\mathrm{h}}^{*}\dot{m}_{\mathrm{c}}^{*})^{y}}{A_{\mathrm{c}}K_{\mathrm{c}}(\dot{m}_{\mathrm{c}}^{*})^{y} + A_{\mathrm{h}}K_{\mathrm{h}}(\dot{m}_{\mathrm{h}}^{*})^{y}} \quad (9)$$

The parameters set from Eq. (5) now becomes

$$\begin{aligned} \alpha(t) &= \alpha^{*}\frac{\dot{m}_{\mathrm{h}}^{*}}{\dot{m}_{\mathrm{h}}(t)}\frac{U(t)}{U^{*}}, \quad & \tau_{\mathrm{h}}(t) &= \tau_{\mathrm{h}}^{*}\frac{\dot{m}_{\mathrm{h}}^{*}}{\dot{m}_{\mathrm{h}}(t)} \\ \beta(t) &= \beta^{*}\frac{\dot{m}_{\mathrm{c}}^{*}}{\dot{m}_{\mathrm{c}}(t)}\frac{U(t)}{U^{*}}, \quad & \tau_{\mathrm{c}}(t) &= \tau_{\mathrm{c}}^{*}\frac{\dot{m}_{\mathrm{c}}^{*}}{\dot{m}_{\mathrm{c}}(t)} \end{aligned} \quad (10)$$

where it is observed that only α and β are affected by the mass flow dependence of U, and that the reference area has cancelled out. Note that in an unknown geometry, there could be two additional parameters to be estimated, the exponents y giving

$$\theta^{*} = \left\{\alpha^{*}, \tau_{\mathrm{h}}^{*}, \beta^{*}, \tau_{\mathrm{c}}^{*}, y_{\mathrm{h}}, y_{\mathrm{c}}\right\}^{\mathrm{T}} \quad (11)$$

3. Parameter estimation

As shown in Jonsson and Palsson [17], the extended Kalman filter is employed to estimate the parameters. As it is desirable to keep as many parameters constant as possible, only α^{*} and β^{*} will be estimated, the last two parameters are computed considering that they represent the median residence time of the fluids in each section during a fixed period of time (here the period when the heat exchanger is not fouled).

By letting α^{*} and β^{*} be model states it is possible to observe the changes in U. Thus, two differential equations are added to the heat exchanger model. Here α^{*} and β^{*} are described as purely random processes, i.e.

$$\frac{\mathrm{d}}{\mathrm{d}t}\begin{bmatrix}\alpha^{*}(t)\\ \beta^{*}(t)\end{bmatrix} = \frac{\mathrm{d}}{\mathrm{d}t}[\underline{\theta}] = \begin{bmatrix}w_{\alpha}(t)\\ w_{\beta}(t)\end{bmatrix} = \underline{w}_{\theta}(t) \quad (12)$$

where $\underline{w}_{\theta}(t)$ is an independent normal distributed white noise process with zero mean and covariance matrix $Q_{\theta}(t)$, i.e. $\underline{w}_{\theta}(t) \in N(\underline{0}, Q_{\theta}(t))$.

The heat exchanger model then becomes (see Eqs. (3) and (12))

$$\frac{\mathrm{d}}{\mathrm{d}t}\begin{bmatrix}\underline{\theta}\\ \underline{T}\end{bmatrix} = \begin{bmatrix}\underline{0}\\ \underline{f}(\dot{\underline{m}}, \underline{T}, \underline{\theta}, \underline{T}_{\mathrm{in}})\end{bmatrix} + \begin{bmatrix}\underline{w}_{\theta}\\ \underline{w}_{\mathrm{f}}\end{bmatrix} \quad (13)$$

Here $\underline{w}_{\mathrm{f}} \approx N(\underline{0}, Q_{\mathrm{f}})$ has been added to Eq. (3) to compensate for deviations from the correct temperature values.

3.1. The extended Kalman filter (EKF)

The type of Kalman filter used (see for example Welch and Bishop [22] for an introduction to Kalman filtering) is the continuous-discrete version of the EKF (e.g. [23]). The model is continuous in time but the measurements are discrete. With $\underline{x} = \begin{bmatrix}\underline{\theta}^{\mathrm{T}} & \underline{T}^{\mathrm{T}}\end{bmatrix}^{\mathrm{T}}$ and $\underline{w} = \begin{bmatrix}\underline{w}_{\theta}^{\mathrm{T}} & \underline{w}_{\mathrm{f}}^{\mathrm{T}}\end{bmatrix}^{\mathrm{T}}$ the Kalman filter equations are (see [23] for more details on the Kalman filter equations):

Model (see Eq. (13))

$$\frac{\mathrm{d}}{\mathrm{d}t}\underline{x}(t) = \begin{bmatrix}\underline{0}\\ \underline{f}(\dot{\underline{m}}, \underline{x}, \underline{T}_{\mathrm{in}})\end{bmatrix} + \underline{w}(t)$$

$$\underline{w} \approx N\left(\underline{0}, \begin{bmatrix}Q_{\theta} & 0\\ 0 & Q_{\mathrm{f}}\end{bmatrix}\right) = N(\underline{0}, Q)$$

Measurement model (extracts the sampled states (the outputs) from the state vector. Measurement noise is added. See H in Eq. (14))

$$\underline{z}_{\mathrm{k}} = H\underline{x}_{k} + \underline{w}_{z,k}, \quad k = 1, 2, \ldots \quad \underline{w}_{z,k} \approx N(0, Q_{z,k})$$

Initial conditions (assume that the initial states are normal distributed. See $\underline{\hat{x}}(0)$ and $P(0)$ in Section 4.2)

$$\underline{x}(0) \approx N(\underline{\hat{x}}(0), P(0))$$

Assumptions (i.e. the state noise and the measurement noise are not correlated)

$$E[\underline{w}(t)\underline{w}_{z,k}^{\mathrm{T}}] = 0 \quad \text{for all } k \text{ and all } t$$

State estimate extrapolation (shows how the estimated states evolve in time)

$$\frac{\mathrm{d}}{\mathrm{d}t}\underline{\hat{x}}(t) = \begin{bmatrix}\underline{0}\\ \underline{f}(\dot{\underline{m}}, \underline{\hat{x}}, \underline{T}_{\mathrm{in}})\end{bmatrix}$$

Error covariance extrapolation (shows how the estimated covariance matrix evolves in time)

$$\frac{\mathrm{d}}{\mathrm{d}t}P(t) = F(\underline{\hat{x}}(t))P(t) + P(t)F(\underline{\hat{x}}(t))^{\mathrm{T}} + Q(t)$$

State estimate update

$$\underline{\hat{x}}_{k}(+) = \underline{\hat{x}}_{k}(-) + K_{k}[\underline{z}_{k} - H\underline{\hat{x}}_{k}(-)]$$

Error covariance update

$$P_{k}(+) = [I - K_{k}H]P_{k}(-)$$

Kalman gain matrix

$$K_{k} = P_{k}(-)H^{\mathrm{T}}[HP_{k}(-)H^{\mathrm{T}} + Q_{z,k}]^{-1}$$

Definition

$$F(\hat{\underline{x}}(t)) = \left.\frac{\partial\begin{bmatrix}\underline{0}\\ \underline{f}(\dot{m},\underline{x},\underline{T}_{\text{in}})\end{bmatrix}}{\partial\underline{x}}\right|(\underline{x}(t)=\hat{\underline{x}}(t))$$

where t stands for continuous time, k stands for the discrete time index, $(-)$ indicates the corresponding values after propagation from t to $t+\Delta t$, $(+)$ denotes values of estimates and covariance of the state estimation errors at time $t+\Delta t$ after measurement and $\wedge$ denotes estimates).

If the measurement matrix (H) is a function of the state variables, a comparable definition to F is used instead. Here however H is constant, for example for the model given by Eq. (13)

$$H = \begin{bmatrix}0 & 0 & 0 & 1 & 0 & 0\\ 0 & 0 & 0 & 0 & 0 & 1\end{bmatrix} \tag{14}$$

That is to say, the measurement matrix extracts the state vector components in $\underline{x}$ which are sampled, i.e. $T_{\text{h},2}$ and $T_{\text{c},2}$ (see Eqs. (13) and (2)).

The extrapolation equations for $\underline{x}$ and P are solved by using 4th and 5th order Runge-Kutta formulas. The selection of values for the system noise covariance matrix Q and measurement noise covariance matrix is in fact part of the problem of estimating the model parameters. Algorithms for estimating the values of Q given Q_z can be found in Jonsson [16]. However, the approach taken here is to try different values for Q with respect to α^* and β^* and study how sensitive the parameter estimates are.

3.2. Calculation of $F(\hat{\underline{x}}(t))$

In this section the calculation of the F matrix is shown. This is in fact a first order Taylor series expansion of the non-linear model about the current estimate of the state vector. Here the heat exchanger model is given by

$$\frac{\mathrm{d}}{\mathrm{d}t}\begin{bmatrix}\alpha^*\\ \beta^*\\ T_{\text{h},1}\\ T_{\text{h},2}\\ T_{\text{c},1}\\ T_{\text{c},2}\end{bmatrix} = \begin{bmatrix}0\\ 0\\ -\frac{1+\alpha/2}{\tau_{\text{h}}}T_{\text{h},1}+\frac{\alpha}{2\tau_{\text{h}}}T_{\text{c},1}+\frac{\alpha}{2\tau_{\text{h}}}T_{\text{c},2}+\frac{1-\alpha/2}{\tau_{\text{h}}}T_{\text{h,in}}\\ \frac{1-\alpha/2}{\tau_{\text{h}}}T_{\text{h},1}-\frac{1+\alpha/2}{\tau_{\text{h}}}T_{\text{h},2}+\frac{\alpha}{2\tau_{\text{h}}}T_{\text{c},1}+\frac{\alpha}{2\tau_{\text{h}}}T_{\text{c,in}}\\ \frac{\beta}{2\tau_{\text{c}}}T_{\text{h},1}+\frac{\beta}{2\tau_{\text{c}}}T_{\text{h},2}-\frac{1+\beta/2}{\tau_{\text{c}}}T_{\text{c},1}+\frac{1-\beta/2}{\tau_{\text{c}}}T_{\text{c,in}}\\ \frac{\beta}{2\tau_{\text{c}}}T_{\text{h},1}+\frac{1-\beta/2}{\tau_{\text{c}}}T_{\text{c},1}-\frac{1+\beta/2}{\tau_{\text{c}}}T_{\text{c},2}+\frac{\beta}{2\tau_{\text{c}}}T_{\text{h,in}}\end{bmatrix}$$

$$+\begin{bmatrix}\underline{w}_\theta\\ \underline{w}_{\text{f}}\end{bmatrix} = \begin{bmatrix}0\\ 0\\ f_1\\ f_2\\ f_3\\ f_4\end{bmatrix} + \begin{bmatrix}\underline{w}_\theta\\ \underline{w}_{\text{f}}\end{bmatrix}$$

then F is the following 6 by 6 matrix

$$F = \begin{bmatrix}0 & 0 & 0 & 0 & 0 & 0\\ 0 & 0 & 0 & 0 & 0 & 0\\ \frac{\partial f_1}{\partial\alpha} & \frac{\partial f_1}{\partial\beta} & \frac{\partial f_1}{\partial T_{\text{h},1}} & \frac{\partial f_1}{\partial T_{\text{h},2}} & \frac{\partial f_1}{\partial T_{\text{c},1}} & \frac{\partial f_1}{\partial T_{\text{c},2}}\\ \frac{\partial f_2}{\partial\alpha} & \frac{\partial f_2}{\partial\beta} & \frac{\partial f_2}{\partial T_{\text{h},1}} & \frac{\partial f_2}{\partial T_{\text{h},2}} & \frac{\partial f_2}{\partial T_{\text{c},1}} & \frac{\partial f_2}{\partial T_{\text{c},2}}\\ \frac{\partial f_3}{\partial\alpha} & \frac{\partial f_3}{\partial\beta} & \frac{\partial f_3}{\partial T_{\text{h},1}} & \frac{\partial f_3}{\partial T_{\text{h},2}} & \frac{\partial f_3}{\partial T_{\text{c},1}} & \frac{\partial f_3}{\partial T_{\text{c},2}}\\ \frac{\partial f_4}{\partial\alpha} & \frac{\partial f_4}{\partial\beta} & \frac{\partial f_4}{\partial T_{\text{h},1}} & \frac{\partial f_4}{\partial T_{\text{h},2}} & \frac{\partial f_4}{\partial T_{\text{c},1}} & \frac{\partial f_4}{\partial T_{\text{c},2}}\end{bmatrix}$$

where

$$\frac{\partial f_1}{\partial\alpha} = \frac{1}{2\tau_{\text{h}}}(T_{\text{c},1}+T_{\text{c},2}-T_{\text{h},1}-T_{\text{h,in}}),$$

$$\frac{\partial f_1}{\partial T_{\text{h},1}} = -\frac{1+\alpha/2}{\tau_{\text{h}}},\quad \frac{\partial f_1}{\partial T_{\text{c},1}} = \frac{\partial f_1}{\partial T_{\text{c},2}} = \frac{\alpha}{2\tau_{\text{h}}},$$

$$\frac{\partial f_2}{\partial\alpha} = \frac{1}{2\tau_{\text{h}}}(T_{\text{c},1}+T_{\text{c,in}}-T_{\text{h},1}-T_{\text{h},2}),$$

$$\frac{\partial f_2}{\partial T_{\text{h},1}} = \frac{1-\alpha/2}{\tau_{\text{h}}},\quad \frac{\partial f_2}{\partial T_{\text{h},2}} = -\frac{1+\alpha/2}{\tau_{\text{h}}},\quad \frac{\partial f_2}{\partial T_{\text{c},1}} = \frac{\alpha}{2\tau_{\text{h}}},$$

$$\frac{\partial f_3}{\partial\beta} = \frac{1}{2\tau_{\text{c}}}(T_{\text{h},1}+T_{\text{h},2}-T_{\text{c},1}-T_{\text{c,in}}),$$

$$\frac{\partial f_3}{\partial T_{\text{h},1}} = \frac{\partial f_3}{\partial T_{\text{h},2}} = \frac{\beta}{2\tau_{\text{c}}},\quad \frac{\partial f_3}{\partial T_{\text{c},1}} = -\frac{1+\beta/2}{\tau_{\text{c}}},$$

$$\frac{\partial f_4}{\partial\beta} = \frac{1}{2\tau_{\text{c}}}(T_{\text{h},1}+T_{\text{h,in}}-T_{\text{c},1}-T_{\text{c},2}),$$

$$\frac{\partial f_4}{\partial T_{\text{h},1}} = \frac{\beta}{2\tau_{\text{c}}},\quad \frac{\partial f_4}{\partial T_{\text{c},1}} = \frac{1-\beta/2}{\tau_{\text{c}}},\quad \frac{\partial f_4}{\partial T_{\text{c},2}} = -\frac{1+\beta/2}{\tau_{\text{c}}},$$

$$\frac{\partial f_1}{\partial\beta} = \frac{\partial f_1}{\partial T_{\text{h},2}} = \frac{\partial f_2}{\partial\beta} = \frac{\partial f_2}{\partial T_{\text{c},2}} = \frac{\partial f_3}{\partial\alpha} = \frac{\partial f_3}{\partial T_{\text{c},2}} = \frac{\partial f_4}{\partial\alpha} = \frac{\partial f_4}{\partial T_{\text{h},2}} = 0$$

4. Results

In the first part, a clean heat exchanger is studied, to determine the influence of the initial values of the Kalman filter, of the sampling period, and of the Q matrix. In the second part, a continuously fouling heat exchanger is studied, and the detection tool is presented.

4.1. The data

The heat exchanger used in the case study is a water to water counterflow tube-in-tube heat exchanger. The inner diameter of the tube (made of stainless steel) separating the cold fluid and the hot fluid is 14 mm. Its outer diameter is 18 mm. The outer diameter of the annulus is 26 mm. The hot fluid is flowing in the inner tube (the cold fluid is then flowing in the annulus). The length of the exchanger is 11 m. The experiments are simulated using a CFD software (namely fluent), in an axisymmetric configuration. The standard $\kappa-\varepsilon$ model [24] is used, as the flow is turbulent in all the studied configurations for both fluids. It has been verified that the time step is short enough with regards to convergence and accuracy. It has been found that 0.5

second is suitable; so that actual time is the sample number divided by two. It has also been verified that the size of the cells is correct (in terms of boundary layer description, and in terms of length/width ratio), and of course that the outlet temperatures during steady states are correctly determined.

Fig. 1 shows the mass flow rates and the inlet temperatures that have been considered for the first part of the study (clean heat exchanger) as they were introduced in the software (using subroutines written in C). Fig. 2 shows the corresponding outlet temperatures as they were obtained by the software. It can be observed that the steady state is never reached.

It has been considered necessary to simulate measurement noise and inaccuracy of the sensors. To do so, a ±2% normally distributed random noise has been added to all values (inputs and outputs). Figs. 3 and 4 show the data that are actually used.

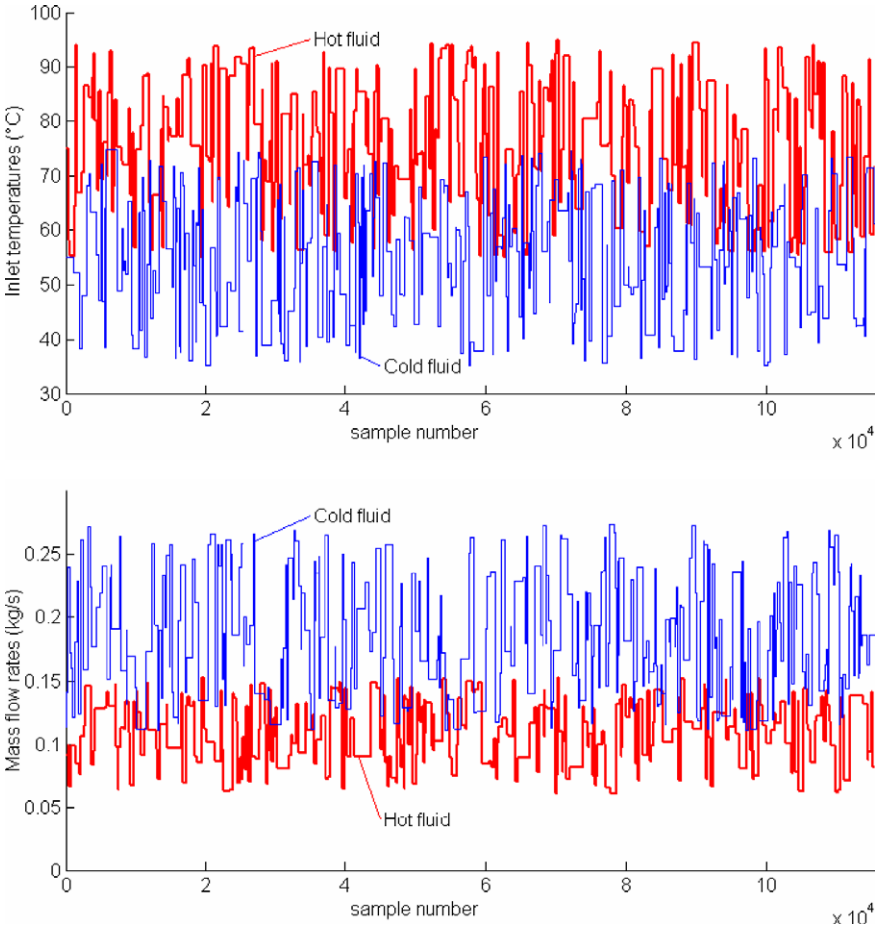

Fig. 1. Inlet temperatures and mass flow rates for hot and cold sides (introduced in the CFD code).

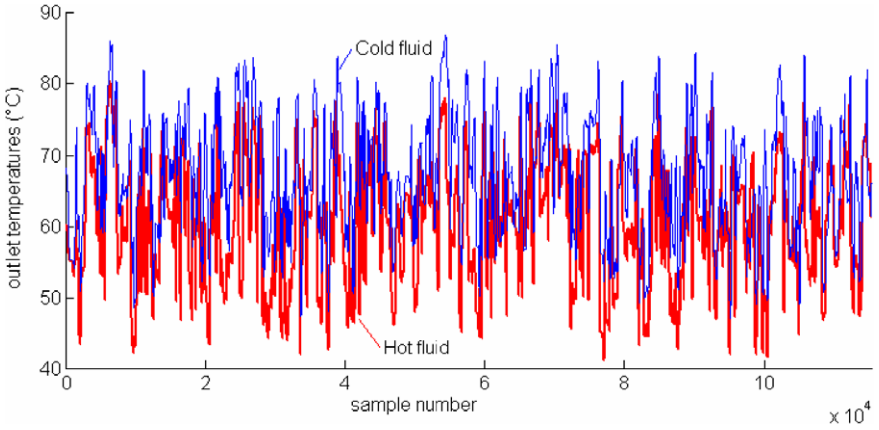

Fig. 2. Outlet temperatures for hot and cold sides (computed by the CFD code).

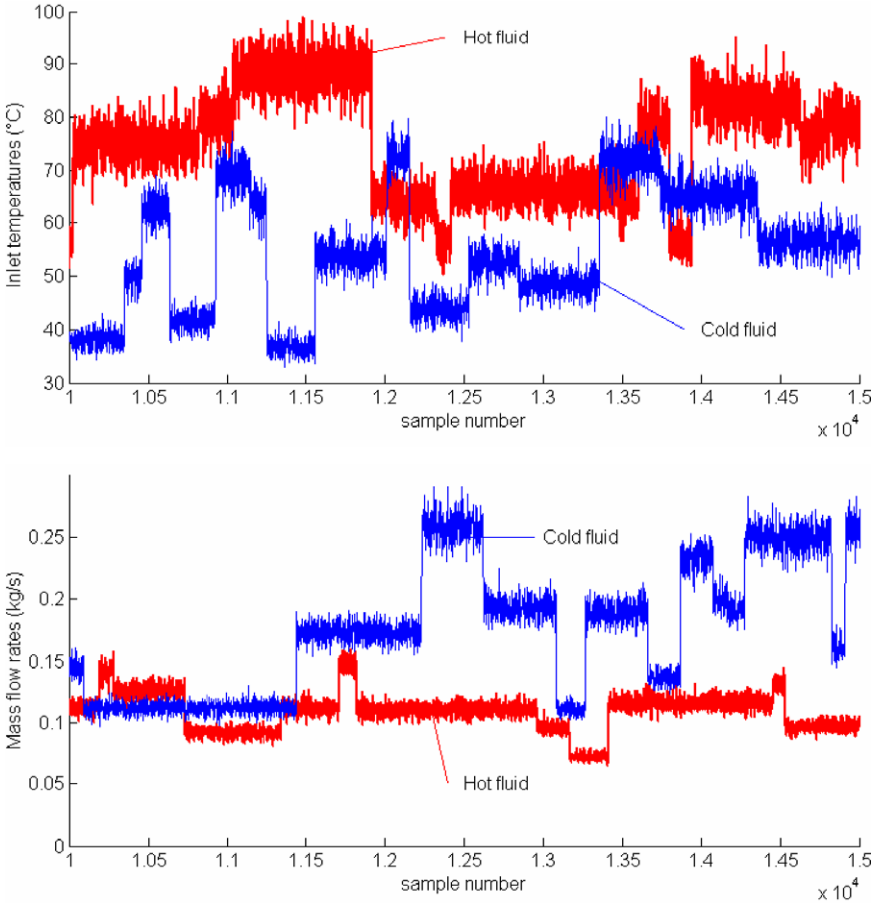

Fig. 3. Inlet temperatures and mass flow rates for hot and cold sides (used for the estimation of the parameters) (partial view).

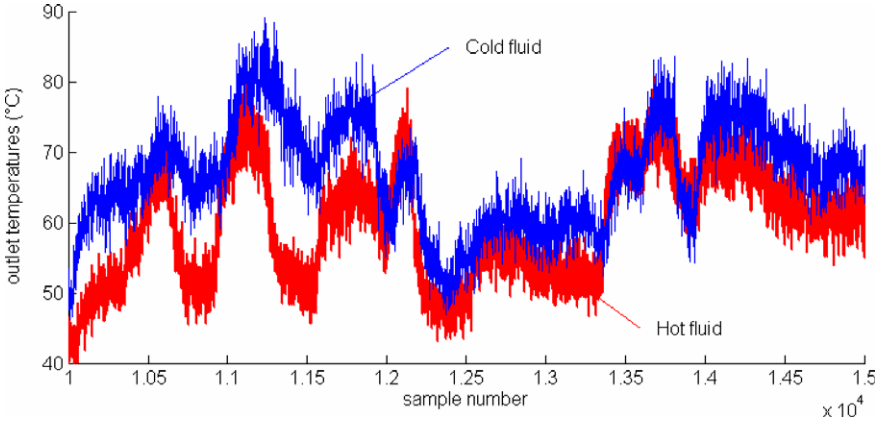

Fig. 4. Outlet temperatures for hot and cold sides (used for the estimation of the parameters) (partial view).

4.2. Starting values for the Kalman filter and model parameters

The following values are common for the Kalman filter and models presented in Sections 3.1 and 3.2

$$Q_z = \begin{bmatrix} 0.1 & 0 \\ 0 & 0.1 \end{bmatrix}, \quad \dot{m}_h^* = 0.1083 \text{ kg/s}, \quad \dot{m}_c^* = 0.1803 \text{ kg/s}$$

Furthermore, the initial values and parameter values in the different models are

$$P(0) = \begin{bmatrix} 0.02^2 & 0 & 0 & 0 & 0 & 0 \\ 0 & 0.02^2 & 0 & 0 & 0 & 0 \\ 0 & 0 & 1 & 0 & 0 & 0 \\ 0 & 0 & 0 & 1 & 0 & 0 \\ 0 & 0 & 0 & 0 & 1 & 0 \\ 0 & 0 & 0 & 0 & 0 & 1 \end{bmatrix}$$

$$\underline{\hat{x}}(0) = \begin{bmatrix} \text{random} \\ \text{random} \\ 74.63\ ^\circ\text{C} \\ 60.07\ ^\circ\text{C} \\ 54.42\ ^\circ\text{C} \\ 72.44\ ^\circ\text{C} \end{bmatrix}, \quad \tau_h^* = 7.7392\text{s},\ \tau_c^* = 8.3502\text{s},\ y = 0.8$$

The first two values of $\underline{\hat{x}}(0)$ are random values ranging from 0 to 2. The above values (for Q_z and P) are based on the results in Jonsson and Palsson [17]. The only undefined value is the Q matrix for the Kalman filter. Generally Q is defined as the diagonal matrix

$$Q = \begin{bmatrix} cI(2 \times 2) & 0(2 \times \text{ns}) \\ 0(\text{ns} \times 2) & 0.1I(\text{ns} \times \text{ns}) \end{bmatrix}$$

where I is the identity matrix, ns is the total number of sections in the model, 0 is the null matrix and c is a variable.

4.3. Clean exchanger

In this first part, a clean heat exchanger is studied. This makes possible the determination of the quasi optimal values of the time step and of the c value. It also makes possible the analysis of the effect of the initial conditions of the Kalman filter.

4.3.1. Role of the Q matrix

In this subsection, the actual time period is 5 s (one out of ten samples is taken into account). Fig. 5 shows the estimation of α^* and β^* for various values of c in the Q matrix. The effects of changing c are obvious. If $c = 10^{-10}$ then the estimation of α^* and β^* is slow and the new equilibrium position is barely reached before the next outlet temperature is reached (e.g. about 2500 samples to reach a correct value for β^*). As c increases, the estimates will result in greater fluctuations about the equilibrium position. For this reason, it is necessary to select c in such a way to insure a sufficiently prompt response while keeping fluctuations to a minimum. It has been chosen to select 10^{-8} as a correct value, so that the filter response is fast enough (about 500 samples), while the fluctuations are small enough.

4.3.2. Influence of the starting values of the filter

Fig. 6 shows the values of α^* and β^* (whole set and the first thousand ones) for a sampling period of 5 s and for 100 random initial conditions ($c = 10^{-8}$). Fig. 7 shows the evolution of the standard deviation of the estimated

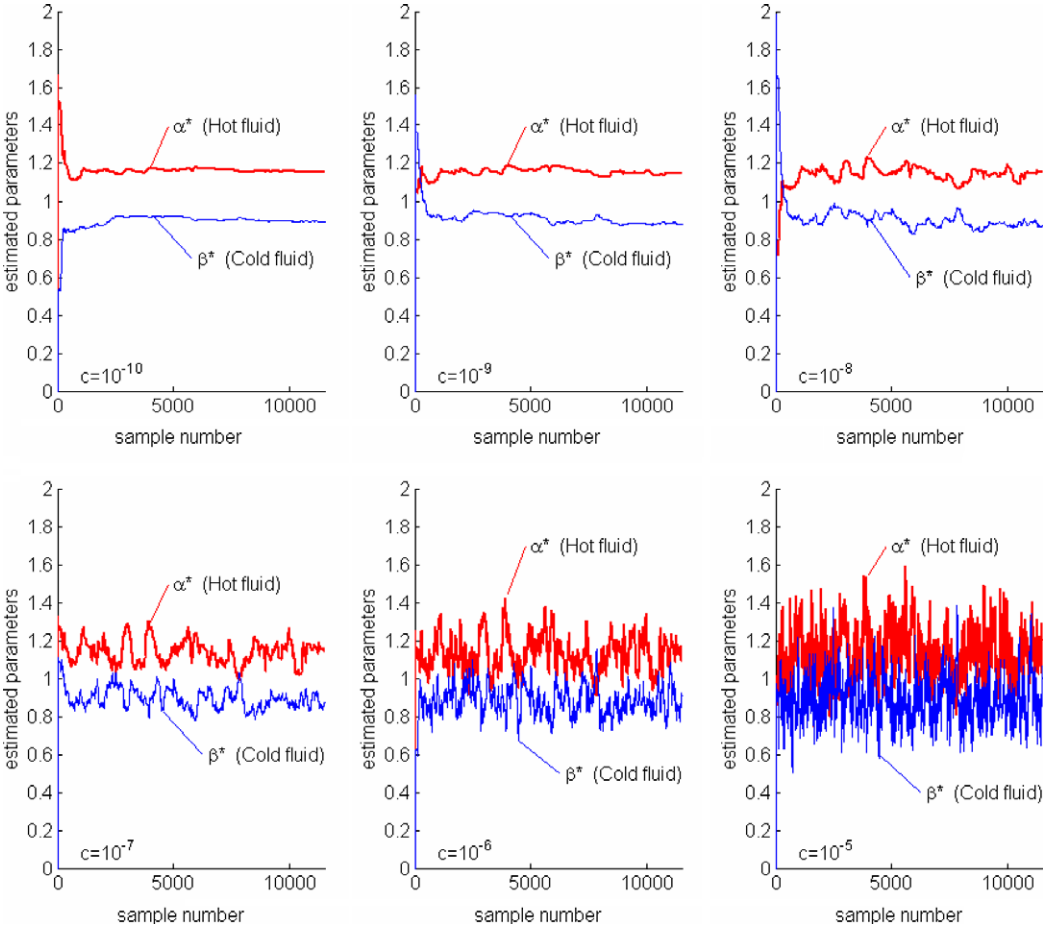

Fig. 5. Estimation of α^* and β^* when c varies from 10^{-10} to 10^{-5}. (Sampling period = 5 s random initial values.)

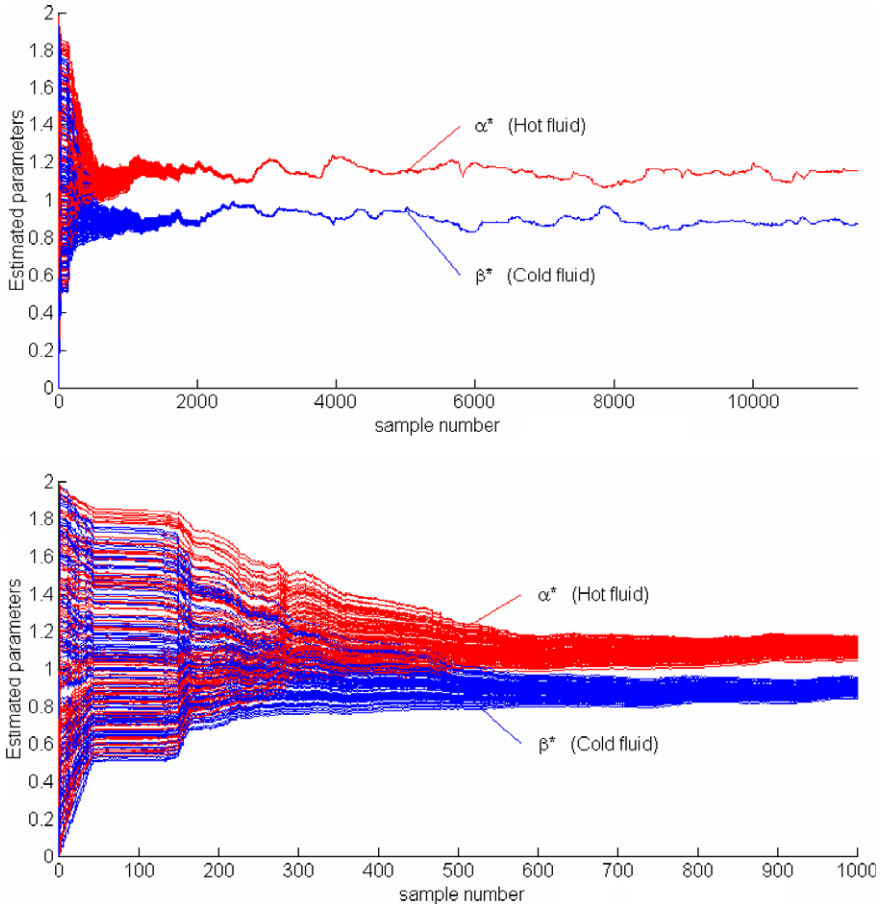

Fig. 6. Values of α^* and β^* for a sampling period of 5 s and for 100 random initial conditions (c is 10^{-8}). (Whole set and the first thousand ones.)

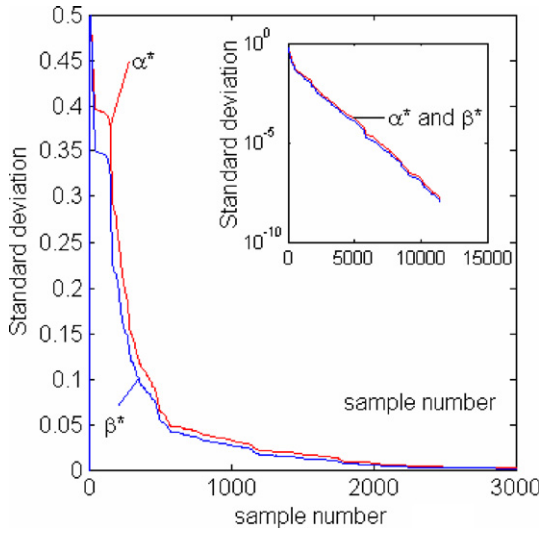

Fig. 7. Evolution of the standard deviation of the estimated values of α^* and β^* for a sampling period of 5 s and for 100 random initial conditions (c is 10^{-8}).

values of α^* and β^* for the same experiment (first 3000 values and for the whole range).

On the one hand, it can be concluded that any random initial values are suitable. On the other hand, it can be concluded that 2000 values have to be estimated (then the standard deviation both for α^* and β^* is less than one percent of the mean value) before the initial values play no longer any significant role (for a sampling period of 5 s, see Section 4.3.3 for the selection of the sampling period). This corresponds to a functioning period of less than three hours. If the user wants a shorter adaptation duration, it is possible to use a shorter sampling rate, as shown in the next section.

4.3.3. Influence of the sampling period

Fig. 8 shows, for random initial values, the mean values of the last twentieth of the values of α^* and β^* for a sampling period ranging from 1 sec (1 sample out of 2 computed samples) to 30 s (1 sample out of 60 computed samples); c is 10^{-8}. It can be concluded that the procedure for the determination of the parameters is very robust. Even though the fluctuations are quite small, it has been chosen to keep a sampling period of 5 s as a good compromise between reactivity and amount of data to be analysed.

4.4. Fouling

In this second part, a continuously fouling heat exchanger is studied. To get the data, the thermal conductivity of

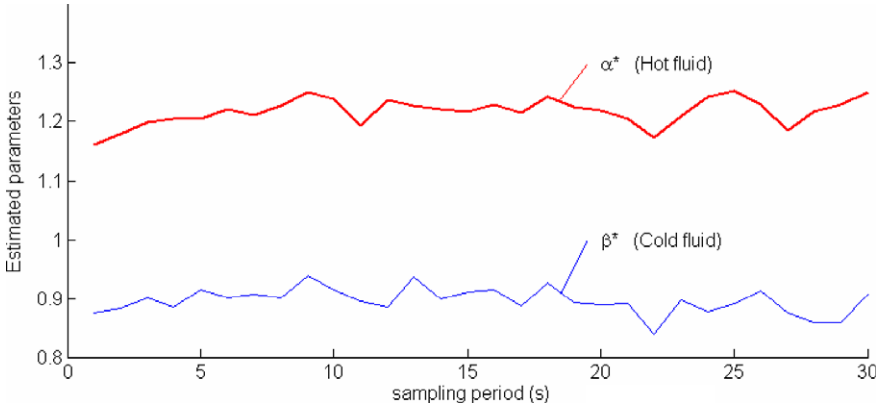

Fig. 8. Mean values of the last tenth of the values of α^* and β^* (c is 10^{-8}).

the inner tube has been continuously decreased (a subroutine is used in the CFD software). The resulting equivalent fouling factor is then computed using:

$$R_f = A_h(R_{th}(t) - R_{th}(0)). \quad (15)$$

This fouling factor is plotted (Fig. 9) versus dimensionless time; the latter is defined as the ratio of the sample number to the total number of samples during the fouling period. It can be seen that the variation is similar to the variation observed (after a slight decrease which is not taken into account here) in e.g. Hays et al. [25] or Fahiminia et al. [26]. Typical values of the fouling factor can be found in Çengel [27], in Incropera and De Witt [20] or at the "engineering webpage" [28]. For water, the fouling factor is typically comprised in the range [0.0001 0.0007]. This interval is smaller than the interval covered by the variation of the thermal conductivity, and corresponds to the [0.663 0.949] interval of the dimensionless time (Fig. 9).

Fig. 10 shows the values of α^* and β^* for two similar drifts when the flow rates and the inlet temperature still randomly vary. The first drift is eight hours long, and the second drift is four hours long; but they both have the same value of the fouling factor for a given dimensionless time. Note that the same clean period is considered before the fouling period to allow for the convergence of the filter (initial values are still random). It can be seen that the evolutions of the parameters are quite similar, having the same range.

A Cusum test, see e.g. Navidi [29], is carried out to detect the drift. This test has been preferred to the Shewhart test due to the fact that it is more sensitive to small shifts, as stated in the NIST online engineering statistics handbook [30]. Due to the fact that fouling leads to the decrease of the estimated parameters, a one-sided test is sufficient (the second side - min operator- of the test would be necessary to detect an increase of the estimated parameters). This test is carried out in two steps:

1) Compute the cumulative sum: $\mathrm{Cus}(k) = \max(0, E[v_{ref}] - E[v] - g\sigma + \mathrm{Cus}(k-1))$,
2) Check if $\mathrm{Cus}(k) > h\sigma$; if so, then the drift is detected.

The moving mean value of the estimated parameters is computed using a number of samples equal to one twentieth of the clean period (see Section 4.3.2). The standard deviation is either the standard deviation of the last twentieth of the clean period or the moving standard deviation.

If g and/or h are too low, false alarms are encountered. If they are too high, the drift is not detected. It has been found that $g = 1.96$ and $h = 1.96$ are a good compromise

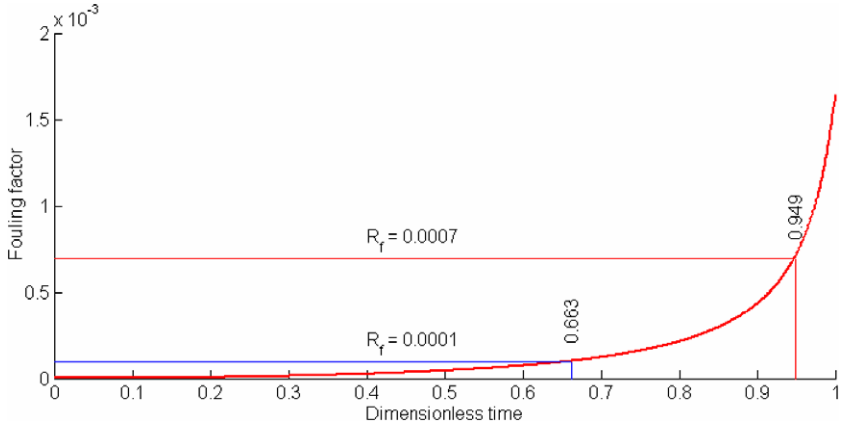

Fig. 9. Fouling factor versus dimensionless time.

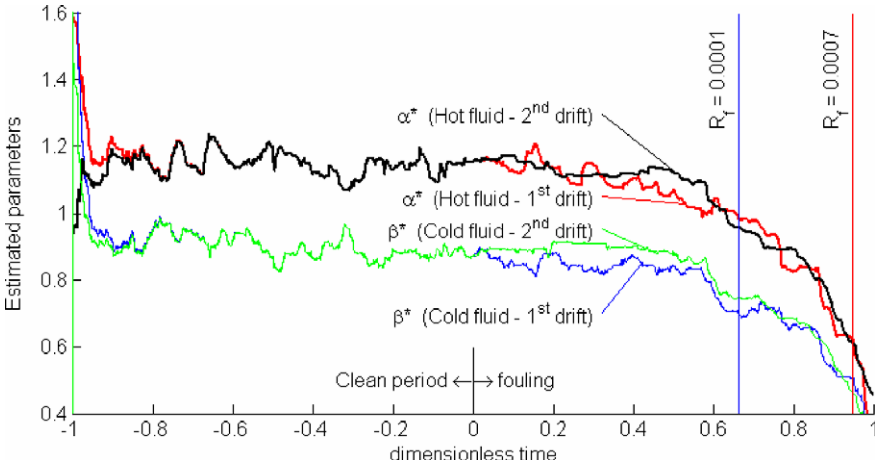

Fig. 10. Values of α^* and β^* for two similar drifts.

(note that 1.96 corresponds to the upper 2.5% tail of the normal $N(0,1)$ distribution, and that, in our case, the test is not very sensitive to the threshold coefficient h).

Fig. 11 shows the values of the cumulative sums for α^* and β^*. The vertical lines are located at the detection dimensionless time. It can be concluded that the drift is detected quite soon, and that the standard deviation of the clean period should be used in the Cusum test. From Fig. 11 it can be seen that a fast drift (second drift) is detected later than a slow drift (first drift). This is due to the fact that the value (see Fig. 5) should be chosen in accordance with the sampling period; itself being chosen in accordance with the speed of the drift. A too small value leads to a longer adaptation time; this is clearly seen on

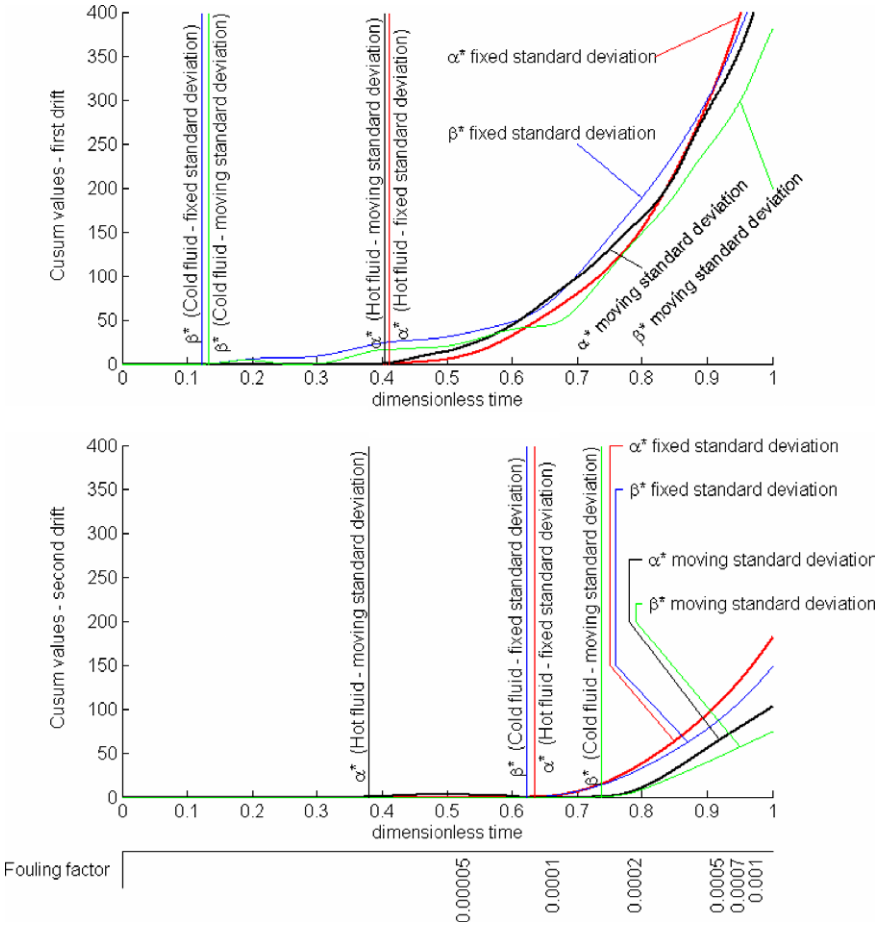

Fig. 11. Cumulative sum tests for α^* and β^* for two similar drifts.

Fig. 10. From what has been done so far, it can be concluded that a minimum of 2000 values are necessary during a clean period and that a sampling period of 1/12,000th of the duration of the drift leads to an early detection.

5. Conclusion

It has been shown how state space models can be applied to detect fouling in heat exchangers. The models are physically based which means that some of their parameters contain the heat transfer coefficients of the heat exchanger. By letting those parameters be time varying, it is possible to follow changes in the heat transfer with time. The model parameters are estimated by using an extended Kalman filter and measurements of inlet and outlet temperatures and the mass flows rates.

In contrast to conventional methods for detecting fouling which require measurements of the heat exchanger operating in steady state this is not the case here. It is sufficient to use measurements from ordinary operation where the load may be changing considerably. It has been shown that the method is not sensitive to the sampling period.

Furthermore, it turns out that the estimates of the model parameters drastically change when quite moderate fouling is introduced. This shows that the method is quite sensitive and in that respect well suited for on-line detection of fouling in heat exchangers.

From the theoretical point of view, future studies will address other configurations such as crossflow heat exchangers, comparisons with other models such as neural networks, and systems such as heat exchanger networks. From the practical point of view, experimental data will be used to confirm the robustness of the method presented here.

Acknowledgements

The authors would like to thank the Research Fund of the University of Iceland for its financial support in this project. This work would have not been carried out without the French/Icelandic Jules Verne program. Hence, the support of Rannís – The Icelandic Centre for Research – and the French Ministry of Foreign Affairs (under Contract EGIDE 12331SJ) is greatly acknowledged.

References

[1] P. Jakobsen, O.B. Stampe, Controlling the Effectiveness of Heat Exchangers. In Danish: Kontrol af varmeveksleres effektivitet). VVS no. 1, vol. 26, 8 January, 1990. ISSN 0042-1944.

[2] T. Casanueva-Robles, T.R. Bott, The environmental effect of heat exchanger fouling: a case study, in: Hans Müller-Steinhagen, M. Reza Malayeri, A. Paul Watkinson (Eds), Proceedings of 6th International Conference on Heat Exchanger Fouling and Cleaning – Challenges and Opportunities, Engineering Conferences International, Kloster Irsee, Germany, June 5–10, 2005, <http://services.bepress.com/eci/heatexchanger2005/>.

[3] H. Poulsen, Fouling in Heat Exchangers in Hot Tap Water Systems. In Danish: Tilsmudsing af varmevekslere i varmt vandssystemer). Department of Heat and Power Engineering, Lund Institute of Technology, Lund, Sweden, 1992. ISBN 91-971587-3-4.

[4] B. Thonon, S. Grandgeorge, C. Jallut, Effect of geometry and flow conditions on particulate fouling in heat exchangers, Heat Transfer Eng. 20 (3) (1999) 12–24.

[5] S.S. Ramachandra, S. Wiehe, M.M. Hyland, X.D. Chen, B. Bansal, A preliminary study of the effect of surface coating on the initial deposition mechanisms of dairy fouling, in: Hans Müller-Steinhagen, M. Reza Malayeri, A. Paul Watkinson (Eds.), Proceedings of 6th International Conference on Heat Exchanger Fouling and Cleaning – Challenges and Opportunities, Editors Engineering Conferences International, Kloster Irsee, Germany, June 5–10, 2005, (<http://services.bepress.com/eci/heatexchanger2005/>).

[6] M.S. Abd-Elhady, C.C.M. Rindt, J.G. Wijers, A.A. van Steenhoven, E.A. Bramer, Th.H. van der Meer, Minimum gas speed in heat exchangers to avoidparticulate fouling, Int. J. Heat Mass Trans. 47 (2004) 943–3955.

[7] M.A.S. Jerónimo, L.F. Melo, A. Sousa Braga, P.J.B.F. Ferreira, C. Martins, Monitoring the thermal efficiency of fouled heat exchangers: a simplified method, Exp. Therm. Fluid Sci. 14 (4) (1997) 455–463.

[8] T.R. Bott, Biofouling control with ultrasound, Heat Transfer Eng. 21 (3) (2000) 43–59.

[9] C. Riverol, V. Naopolitano, Estimation of the overall heat transfer coefficient in a tubular heat exchanger under fouling using neural networks. Application in a flash pasteurizer, Int. Commun. Heat Mass Trans. 29 (4) (2002) 453–457.

[10] C. Riverol, V. Naopolitano, Estimation of fouling in a plate heat exchanger through the application of neural networks, J. Chem. Technol. Biotechnol. 80 (2005) 594–600.

[11] X.D. Chen, X.Y.L. Lin, S.X.Q. Lin, N. Özkan, On-line fouling/cleaning detection by measuring electrical resistance, in: Proceedings of the International Meeting Fouling, Cleaning and Disinfection in Food Processing, Jesus College, Cambridge, UK, 3–5 April 2002, pp. 235–244.

[12] P.K. Nema, A.K. Datta, A computer based solution to check the drop in milk outlet temperature due to fouling in a tubular heat exchanger, J. Food Eng. 71 (2005) 133–142.

[13] M.M. Prieto, J. Miranda, B. Sigales, Application of a step-wise method for analysing fouling in shell-and-tube exchangers, Heat Transfer Eng. 20 (4) (1999) 19–26.

[14] M.M. Prieto, J.M. Vallina, I. Suárez, I. Martin, Application of a design code for estimating fouling on-line in a power plant condenser refrigerated by seawater, in: Proceedings of the ASME-ZSITS International Thermal Science Seminar, Bled, Slovenia, on CD-ROM, 2000.

[15] G.R. Jónsson, J. Holst, Statistical parameter estimation of a counter flow heat exchanger, International Symposium on District Heat Simulation, Reykjavík, Iceland, 13–16. April 1989.

[16] G.R. Jónsson, Parameter estimation in models of heat exchangers and geothermal reservoirs. PhD thesis, Department of Mathematical Statistics, Lund Institute of Technology, Lund, Sweden, 1990.

[17] G.R. Jónsson, O.P. Palsson, An Application of Extended Kalman Filtering to Heat Exchanger Models, J. Dyn. Sys., Measure. Contr. 116 (June) (1994) 257–264.

[18] J.W. Palen, Heat Exchanger Sourcebook, Hemisphere Publishing Corporation, Washington, 1986.

[19] J. Padet, Echangeurs thermiques, methods globales de calcul avce 11 problèmes résolus, Masson, Paris, 1994.

[20] F.P. Incropera, D.P. DeWitt, Fundamentals of Heat and Mass Transfer, fifth ed., John Wiley & Sons, 2001.

[21] G. Jónsson, O.P. Palsson, K. Sejling, Modeling and parameter estimation of heat exchangers – A statistical approach, J. Dyn. Sys., Measure. Contr. 114 (December) (1992) 673–679.

[22] G. Welch, G. Bishop, An introduction to the Kalman filter, <http://www.cs.unc.edu/~welch/media/pdf/kalman_intro.pdf>, updated July 24, 2006.

[23] A. Gelb, Applied Optimal Estimation, MIT Press, Cambridge, Massachusetts, USA, 1974.

[24] B.E. Launder, D.B. Spalding, Lectures in Mathematical Models of Turbulence, Academic Press, London, 1972.
[25] G.F. Hays, E.S. Beardwood, S.J. Colby, Enhanced heat exchange tubes: their fouling tendency and potential cleanup, in: Hans Müller-Steinhagen, M. Reza Malayeri, A. Paul Watkinson (Eds.), Proceedings of 6th International Conference on Heat Exchanger Fouling and Cleaning – Challenges and Opportunities, Engineering Conferences International, Kloster Irsee, Germany, June 5–10, 2005, <http://services.bepress.com/eci/heatexchanger2005/>.
[26] F. Fahiminia, A.P. Watkinson, N. Epstein, Calcium sulphate scaling delay times under sensible heating conditions, in: Hans Müller-Steinhagen, M. Reza Malayeri, A. Paul Watkinson (Eds.), Proceedings of 6th International Conference on Heat Exchanger Fouling and Cleaning – Challenges and Opportunities, Engineering Conferences International, Kloster Irsee, Germany, June 5–10, 2005, <http://services.bepress.com/eci/heatexchanger2005/>.
[27] Y.A. Çengel, Introduction to Thermodynamics and Heat Transfer, Irwin/McGraw-Hill, 1997.
[28] <http://www.engineeringpage.com/technology/thermal/fouling_factors.html>.
[29] W. Navidi, Statistics for Engineers and Scientists, McGraw-Hill International Edition, New York, USA, 2006.
[30] NIST/SEMATECH, 2006, e-Handbook of Statistical Methods, 2006, <http://www.itl.nist.gov/div898/handbook/>.